[Supplemental Data: RNA/2008/009936 (REVISED)]

A Complex RNA Motif Defined By Three Discontinuous 5-Nucleotide-Long Strands Is Essential for Flavivirus RNA Replication†

Byung-Hak Song,[1] Sang-Im Yun,[1] Yu-Jeong Choi,[1] Jeong-Min Kim,[1]
Chan-Hee Lee,[2] and Young-Min Lee[1*]

[1]Department of Microbiology, College of Medicine and Medical Research Institute,
Chungbuk National University, Cheongju, South Korea
[2]Division of Life Sciences, College of Natural Sciences and Research Institute for Genetic Engineering,
Chungbuk National University, Cheongju, South Korea

- Manuscript:
  - Total Number of Text Pages: 49
  - Total Number of Words in Abstract: 259
  - Total Number of Tables: 1
  - Total Number of Figures: 10
- Supplemental Data:
  - Text File with One Table and Seven Figures

Running title: Multiple Base-Pairings in JEV Genome Replication

* Corresponding author: Department of Microbiology
College of Medicine & Medical Research Institute
Chungbuk National University
12 Gaeshin-Dong, Heungduk-Ku
Cheongju-Si, South Korea
Phone : +82-43-261-2863
Fax : +82-43-272-1603
E-mail : ymlee@chungbuk.ac.kr

† Supplemental materials for this article are provided separately.

FIGURE LEGENDS

FIGURE S1. Effect on genome RNA replication of substituting C_{-5} in the R strand of LRM. (**A**) The TDCS motifs for the WT, LRM, and three LRM derivatives bearing a single nucleotide substitution of C_{-5} with U (LRM/Rev3, as described in Fig. 5), A (LRM/C_{-5}A), or G (LRM/C_{-5}G). The altered nucleotides are shown in black boldface type. (**B**) Specific infectivities of the synthetic RNAs transcribed from each cDNA and representative focus morphologies. Naïve BHK-21 cells were transfected with 2 μg of WT, LRM, or one of three LRM-derivative RNAs transcribed from each cDNA, as indicated. At 4 days after transfection, the specific infectivities of the synthetic RNA transcripts were estimated by infectious center assays (**B**, Infectivity); the infectious centers of foci were visualized by immunostaining of the transfected cells with a mouse JEV-specific hyperimmune antiserum (**B**, Representative foci).

FIGURE S2. Schematic presentation of the base-pairing interaction predicted between the M strand of 3'M-R duplex and an alternative 5'L (L^{Alt}) strand in three LRM-derived pseudorevertants. Three novel sequences (LRM/Rev1, LRM/Rev2, and LRM/Rev3) discovered in LRM-derived pseudorevertants are indicated in black boldface type. Also highlighted schematically are predicted nucleotide sequences and relative locations of the three strands (one of either L or L^{Alt}, M, and R) of the TDCS formed by WT, LRM, and LRM derivatives containing one of the three novel sequences, and their potential base-pairing patterns.

FIGURE S3. Effect on genome RNA replication of substituting U_{-81} in the M strand of MMR. (**A**) The TDCS motifs for the WT, MMR, and three MMR derivatives harboring a single nucleotide substitution of U_{-81} with C (MMR/Rev1, as described in Fig. 6), A (MMR/U_{-81}A), or G (MMR/U_{-81}G). The altered nucleotides are shown in black boldface type. (**B**) Specific infectivities of the synthetic RNAs transcribed

from each cDNA and representative focus morphologies. Experiments were performed as described for Fig. S1. ND, not detected.

FIGURE S4. Effect on genome RNA replication of substituting A_{-82} in the M strand of MMR. (**A**) The TDCS motifs for the WT, MMR, and three MMR derivatives containing a single nucleotide substitution of A_{-82} with U (MMR/Rev2, as described in Fig. 6), G (MMR/A_{-82}G), or C (MMR/A_{-82}C). The altered nucleotides are shown in black boldface type. (**B**) Specific infectivities of the synthetic RNAs transcribed from each cDNA and representative focus morphologies. Experiments were performed as described for Fig. S1.

FIGURE S5. Schematic presentation of the base-pairing interaction predicted between the M strand of 3'M-R duplex and an alternative 5'L ($L1^{Alt}$ or $L2^{Alt}$) strand in each of two MMR-derived pseudorevertants. Two point mutations (MMR/Rev1 and MMR/Rev2) acquired in MMR-derived pseudorevertants are shown in black boldface type. Also illustrated schematically are predicted nucleotide sequences and relative locations of the three strands (one of either L, $L1^{Alt}$, or $L2^{Alt}$, M, and R) of the TDCS formed by WT, MMR, and MMR derivatives containing one of the two point mutations, and their potential base-pairing patterns.

FIGURE S6. Effect on genome RNA replication of inserting the R-strand sequence into the site of either the $L1^{Alt}$ or $L2^{Alt}$ deletion in two MMR derivatives, MMR/Rev1/$\Delta L1^{Alt}$ and MMR/Rev2/$\Delta L2^{Alt}$. (**A**) The TDCS motifs formed by each RNA, as illustrated in Fig. 6. (**B**) The specific infectivities and representative focus morphologies generated with each RNA, as indicated. Insertion of the R-strand sequence (5'-AGGAU-3') into the site of either the $L1^{Alt}$ or $L2^{Alt}$ deletion in the two MMR derivatives (MMR/Rev1/$\Delta L1^{Alt}$ and MMR/Rev2/$\Delta L2^{Alt}$) was sufficient to produce phenotypic reversion to high RNA infectivity and a homogeneous focus morphology. Experiments were performed as described for Fig. S1.

FIGURE S7. Schematic presentation of the base-pairing interaction predicted between the M strand of 3'M-R duplex and an alternative 5'L (L^{Alt}) strand in two pseudorevertants originating from LLR and LRR. Indicated in black boldface type is an identical novel sequence of the five nucleotides ($U_{-7}U_{-6}U_{-5}U_{-4}A_{-3}$) that was discovered in the R strand of the TDCS in two pseudorevertants originating from LLR (LLR/Rev) and LRR (LRR/Rev). Also presented schematically are predicted nucleotide sequences and relative locations of the three strands (one of either L or L^{Alt}, M, and R) of the TDCS formed by each RNA, as indicated, and their potential base-pairing patterns.

TABLE S1. Summary of 17 novel sequences acquired in LMM-derived pseudorevertants.

Groups[a]	Clones	Sequences[b]
	WT	AAGAACACAGGAUCU-3'
	LMM	AAGAACACUUCUACU-3'
I	LMM/Rev1	AAGAACACUUCUACAAAGAUCU-3'
I	LMM/Rev2	AAGAACACUUCUACAAGAUCU-3'
I	LMM/Rev3	AAGAACACUUCUACUAGAUCU-3'
I	LMM/Rev4	AAGAACACUUCUACAGAUCU-3'
II	LMM/Rev5	AAGAACACUU-UAGAUCU-3'
II	LMM/Rev6	AAGAACACUUC--GAUCU-3'
II	LMM/Rev7	AAGAACACUU--AGAUCU-3'
II	LMM/Rev11	AAGAACACUU---GAUCU-3'
II	LMM/Rev12	AAGAACACU----GAUCU-3'
II	LMM/Rev14	AAGAACAC-----GAUCU-3'
III	LMM/Rev8	AAGAACA-UU--AUAUCU-3'
III	LMM/Rev13	AAGAACAC---UAUAUCU-3'
IV	LMM/Rev9	AAGAACACUU--GUAUCU-3'
IV	LMM/Rev10	AAGAACACUU--GAAUCU-3'
V	LMM/Rev15	AAGAACA----GUUAUCU-3'
V	LMM/Rev16	AAGAACA-----GAAUCU-3'
V	LMM/Rev17	AAGAACA-----GUAUCU-3'

[a] 17 novel sequences (LMM/Rev1 to 17) acquired in LMM-derived pseudorevertants are classified into five groups, I to V.

[b] The altered nucleotides in LMM are indicated in blue.

Nucleotide sequence of the 3'-end region of LMM-derived pseudorevertants was determined by 3' rapid amplification of cDNA ends.

Novel nucleotide sequences that were acquired in LMM-derived pseudo-revertants are shown in red. Hyphens indicate the deleted nucleotide sequences in the parental LMM.

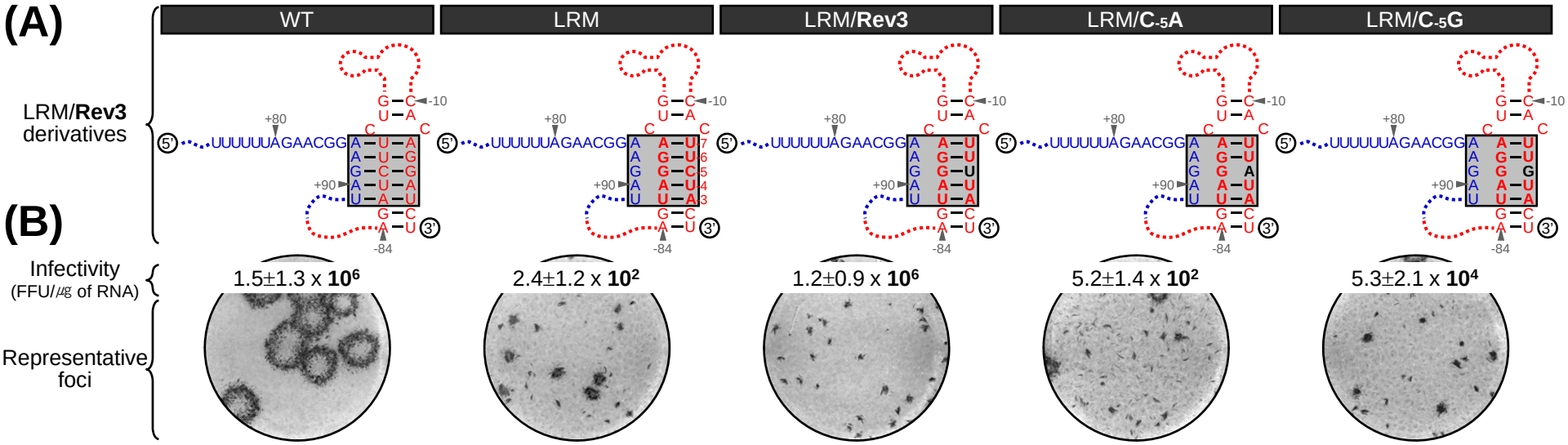

Figure S1. Song et al., 2008

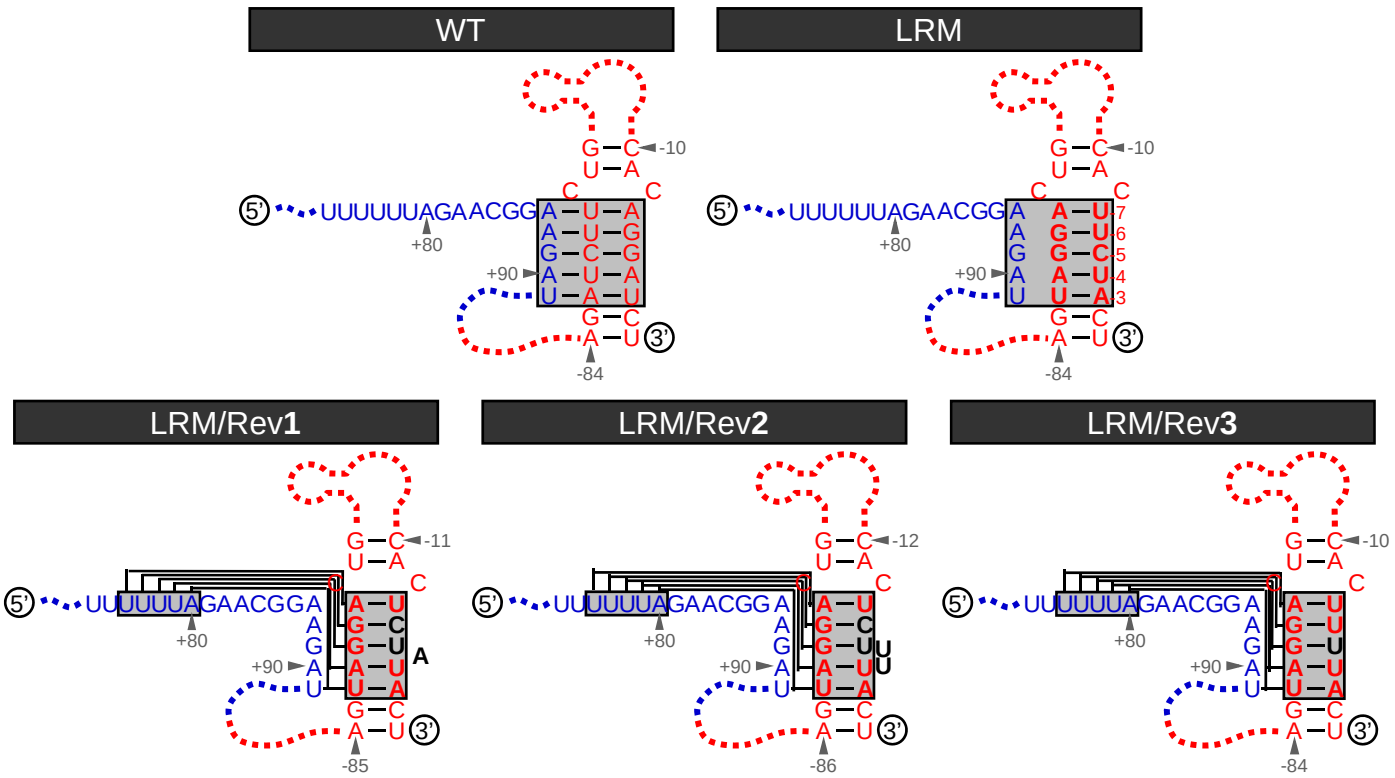

Figure S2. Song et al., 2008

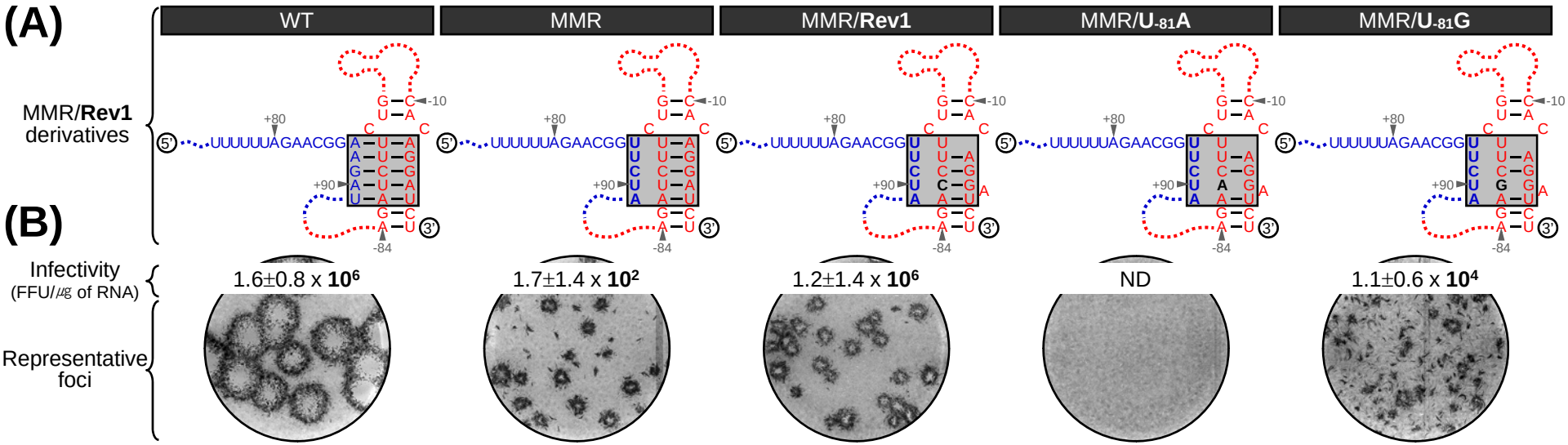

Figure S3. Song et al., 2008

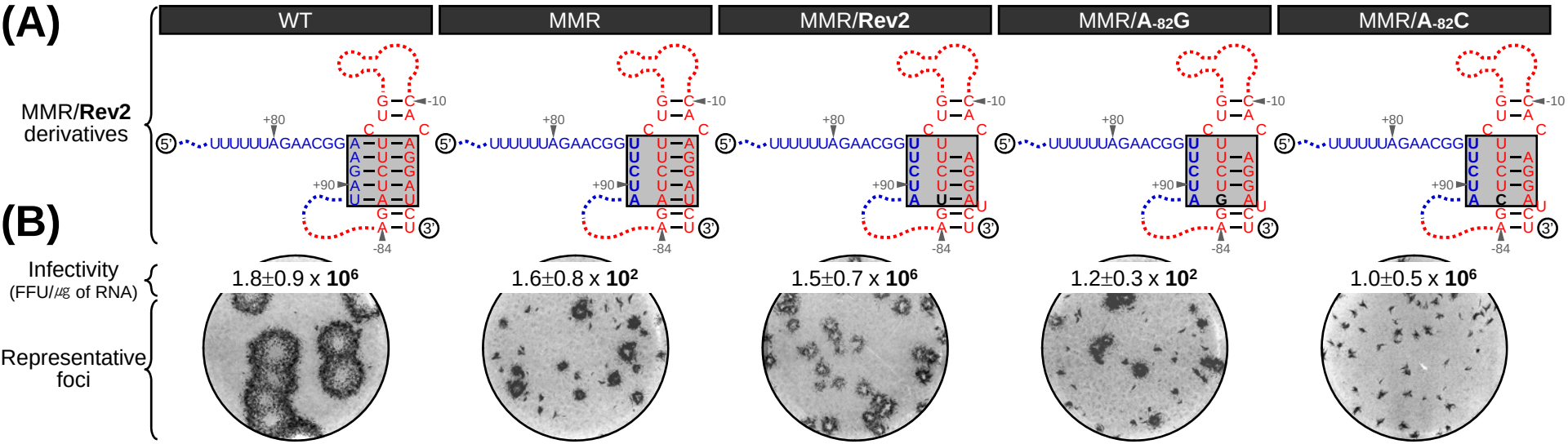

Figure S4. Song et al., 2008

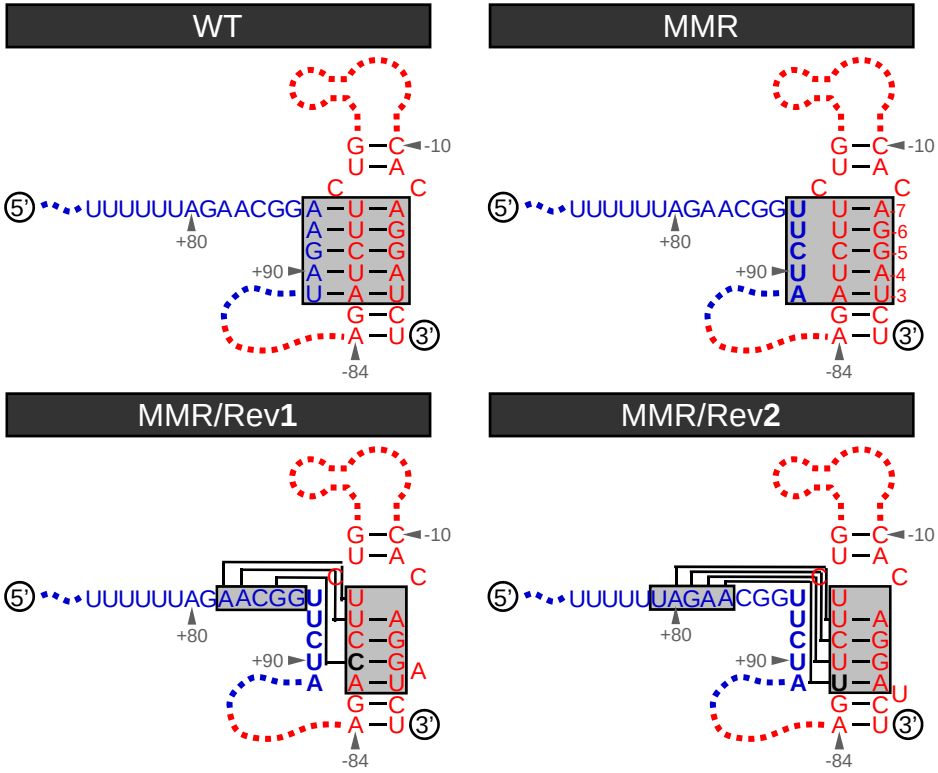

Figure S5. Song et al., 2008

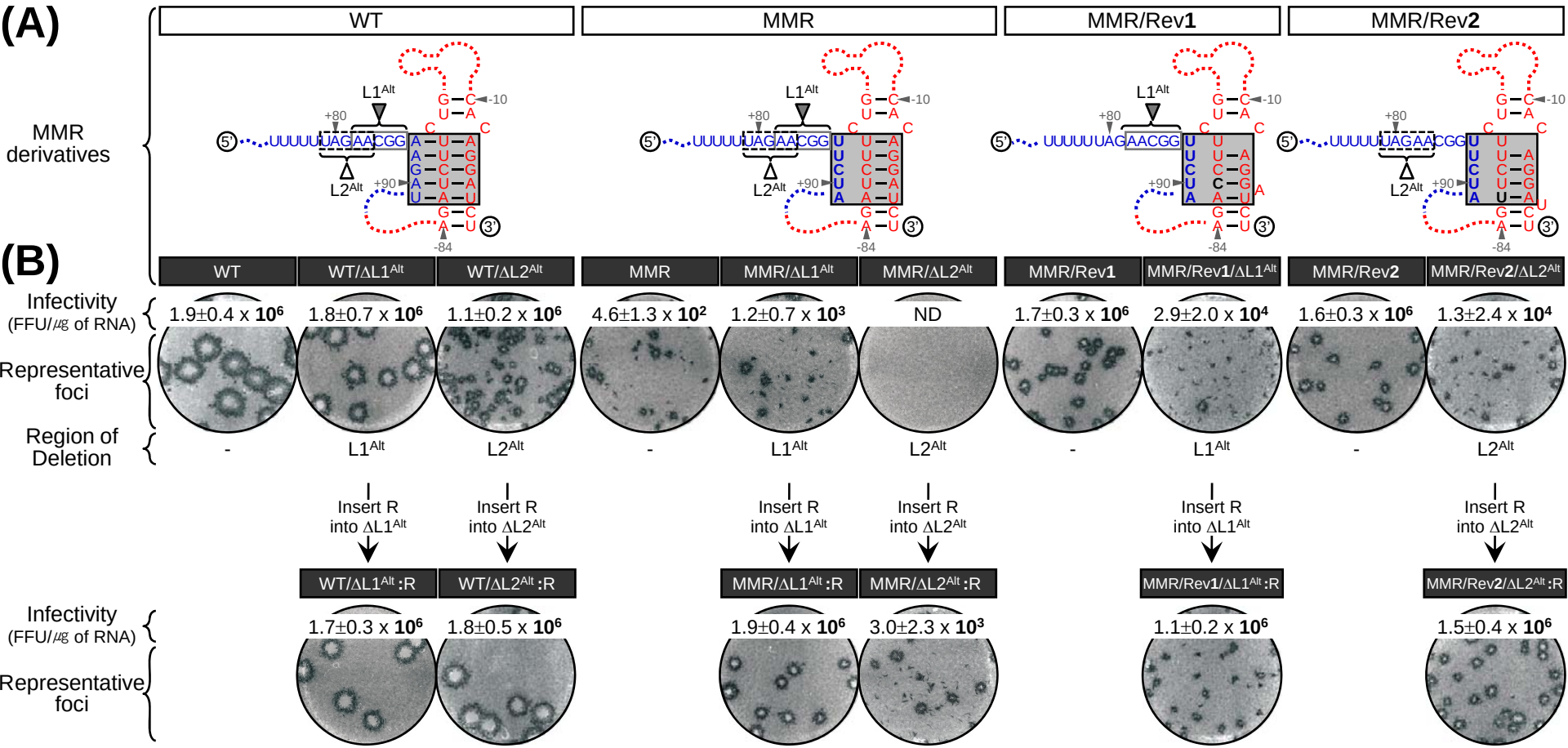

Figure S6. Song et al., 2008

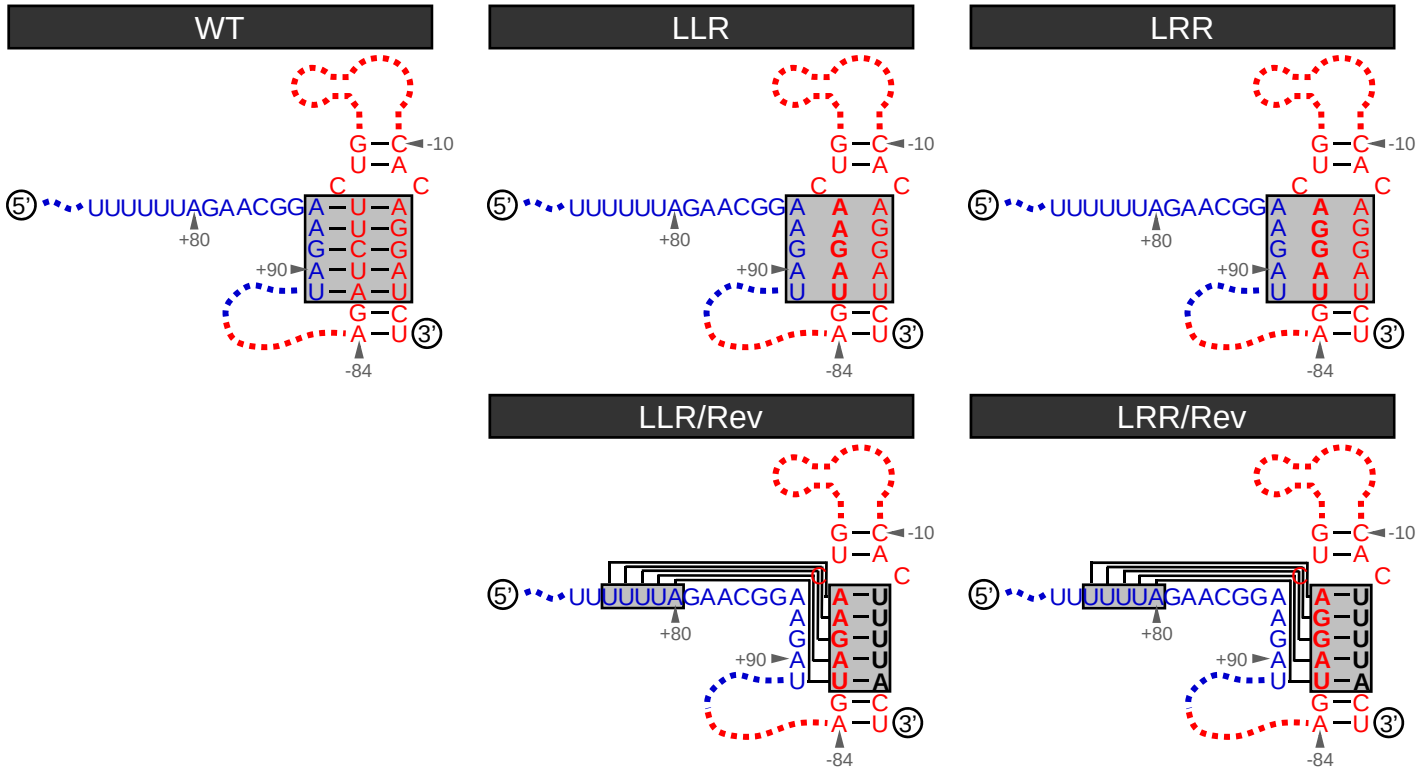

Figure S7. Song et al., 2008